Electronic Supplementary Material (ESI) for New Journal of Chemistry.
This journal is © The Royal Society of Chemistry and the Centre National de la Recherche Scientifique 2022

Supporting Information

Two porous three-dimensional (3D) metal-organic frameworks based on diverse metal clusters: selective sensing of Fe^{3+} and $Cr_2O_7^{2-}$

Yang-Tian Yan [a,*], Yun-Long Wu [a], Li-Na Zheng [a], Wei Cai [a], Peng-Fei Tang [a], Wei-Ping Wu [c], Wen-Yan Zhang [b], and Yao-Yu Wang [b]

[a] School of Materials Science & Engineering, Xi'an Polytechnic University, Xi'an 710048, P. R. China.

[b] Key Laboratory of Synthetic and Natural Functional Molecule of Ministry of Education, Shaanxi Key Laboratory of Physico-Inorganic Chemistry, College of Chemistry & Materials Science, Northwest University, Xi'an 710127, P. R. China.

[c] College of Chemistry and Environmental Engineering and Key Laboratory of Green Chemistry of Sichuan Institutes of Higher Education, Sichuan University of Science and Engineering, Zigong 643000, P. R. China.

Table S1 Crystallographic data and Structural Refinement Parameters of **1** and **2**.

MOFs	**1**	**2**
formula	$C_{59}H_{65}Zn_5N_5O_{29}$	$C_{66}H_{88}Cu_3N_8O_{29}$
*M*r	1635.01	1648.06
crystal system	triclinic	orthorhombic
space group	*P*-1	*Imma*
a (Å)	12.153(2)	30.462(4)
b (Å)	12.643(3)	28.777(4)
c (Å)	12.690(3)	12.1091(17)
α (º)	84.243(3)	90
β (º)	85.337(3)	90
γ (º)	78.012(3)	90
V (Å^3)	1894.1(7)	10615(3)
Z	1	4
D_{calc}(g cm^{-3})	1.433	1.031
F(000)	836.0	3436.0
GOF on F^2	1.087	0.945
R_1[a] [I>2σ(I)]	0.0549	0.0482
wR_2[b] (all data)	0.1913	0.1234

[a] $R_1 = \Sigma||F_o| - |F_c||/\Sigma|F_o|$, wR_2[b]$=[\Sigma w(F_o^2-F_c^2)^2/\Sigma w(F_o^2)^2]^{1/2}$

Table S2. Selected Bond Length (Å) and Angles (°) for 1 and 2

Complex 1			
O(1)-Zn(2)#1	1.909(4)	Zn(1)-O(3)#2	2.060(3)
Zn(1)-O(3)	2.060(3)	Zn(1)-O(6)#2	2.181(4)
Zn(1)-O(6)	2.181(4)	O(9)-Zn(3)#6	1.931(4)
Zn(1)-O(8)#2	2.041(4)	O(10)-Zn(2)#4	2.001(4)
Zn(1)-O(8)	2.041(4)	O(11)-Zn(3)#4	1.953(4)
Zn(2)-O(1)#3	1.909(4)	O(3)-Zn(1)-O(3)#2	180.0
Zn(2)-O(3)	1.974(4)	O(3)-Zn(1)-O(6)	96.03(15)
Zn(2)-O(4)	1.966(4)	O(3)-Zn(1)-O(6)#2	83.97(15)
Zn(2)-O(10)#4	2.001(4)	O(3)#2-Zn(1)-O(6)	83.97(15)
Zn(3)-O(3)	1.973(4)	O(3)#2-Zn(1)-O(6)#2	96.03(15)
Zn(3)-O(7)	1.929(4)	O(6)-Zn(1)-O(6)#2	180.0(2)
Zn(3)-O(9)#5	1.931(4)	O(1)#3-Zn(2)-O(3)	109.31(16)
Zn(3)-O(11)#4	1.953(4)	O(1)#3-Zn(2)-O(4)	117.78(18)
O(8)-Zn(1)-O(3)#2	88.97(17)	O(11)#4-Zn(3)-O(3)	105.83(17)
O(8)-Zn(1)-O(3)	91.03(17)	O(3)-Zn(2)-O(10)#4	108.39(16)
O(8)#2-Zn(1)-O(3)#2	91.03(17)	O(4)-Zn(2)-O(3)	115.58(17)
O(8)#2-Zn(1)-O(3)	88.97(17)	O(4)-Zn(2)-O(10)#4	99.6(2)
O(8)-Zn(1)-O(6)	89.80(16)	O(7)-Zn(3)-O(3)	110.82(17)
O(8)-Zn(1)-O(6)#2	90.20(16)	O(7)-Zn(3)-O(9)#5	121.5(2)
O(8)#2-Zn(1)-O(6)	90.20(16)	O(7)-Zn(3)-O(11)#4	103.5(2)
O(8)-Zn(1)-O(8)#2	180.0	O(9)#5-Zn(3)-O(3)	106.20(18)
Symmetrical codes: #1 x, y+1, z; #2 -x, -y+1, -z+1; #3 x, y-1, z; #4 -x+1, -y+1, -z+1; #5 x, y, z-1; #6 x, y, z+1 for **1**			
Complex 2			
Cu(1)-O(1)	1.9447(17)	Cu(2)-O(3)	1.9744(18)
Cu(1)-O(1)#1	1.9448(17)	Cu(2)-O(4)#4	1.9716(19)
Cu(1)-O(1)#2	1.9448(17)	Cu(2)-O(4)#6	1.9716(19)
Cu(1)-O(1)#3	1.9448(17)	Cu(2)-O(5)	2.155(4)
Cu(2)-O(3)#5	1.9743(18)	O(4)-Cu(2)#4	1.9716(19)
O(1)-Cu(1)-O(1)#2	180.0	O(3)#5-Cu(2)-O(3)	88.98(12)
O(1)#2-Cu(1)-O(1)#1	88.52(10)	O(3)-Cu(2)-O(5)	95.48(11)
O(1)#2-Cu(1)-O(1)#3	91.48(10)	O(3)#5-Cu(2)-O(5)	95.48(11)
O(1)#3-Cu(1)-O(1)#1	180.00(8)	O(4)#4-Cu(2)-O(3)#5	90.05(9)
O(1)-Cu(1)-O(1)#1	91.48(10)	O(4)#6-Cu(2)-O(3)	90.05(9)

O(1)-Cu(1)-O(1)#3	88.52(10)	O(4)#6-Cu(2)-O(3)#5	168.41(9)
O(4)#4-Cu(2)-O(3)	168.41(9)	O(4)#6-Cu(2)-O(5)	96.11(10)
O(4)#4-Cu(2)-O(4)#6	88.58(12)	O(4)#4-Cu(2)-O(5)	96.11(10)

Symmetrical codes: #1 -x+1/2, y+0, -z+3/2; #2 -x+1/2, -y-1/2, -z+3/2; #3 x, -y-1/2, z; #4 -x+1, -y, -z+1; #5 -x+1, y, z; #6 x, -y, -z+1 **for 2**

Fig. S1. The structure of **1** in ellipsoid model (**a**) and coordination configuration of H_5L ligand in **1** (**b**).

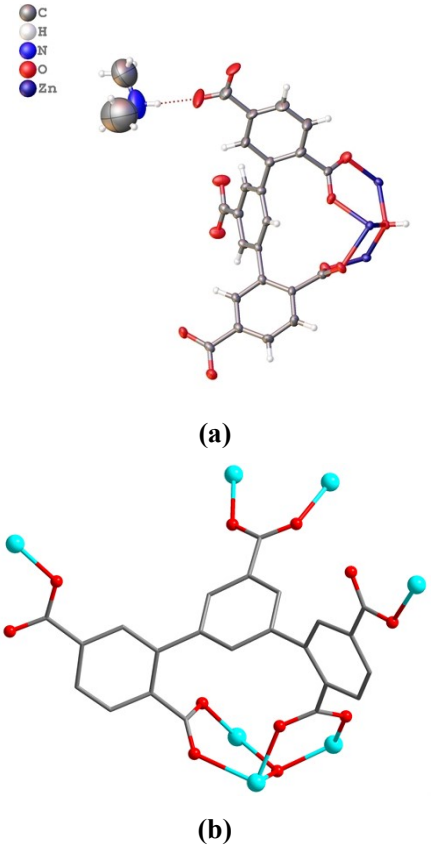

(a)

(b)

Fig. S2. 3D microporous framework of **1** and along *a*-axis. All the H atoms and guest molecules are omitted for clarity.

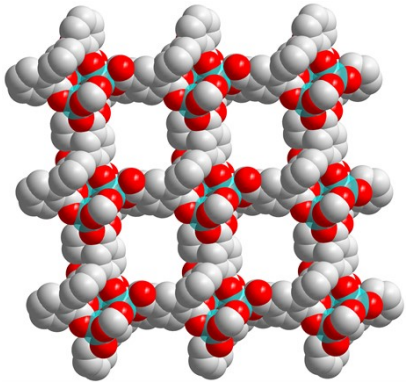

Fig. S3. The structure of **2** in ellipsoid model (**a**) and coordination configurations of H_5L ligand in **2** (**b**).

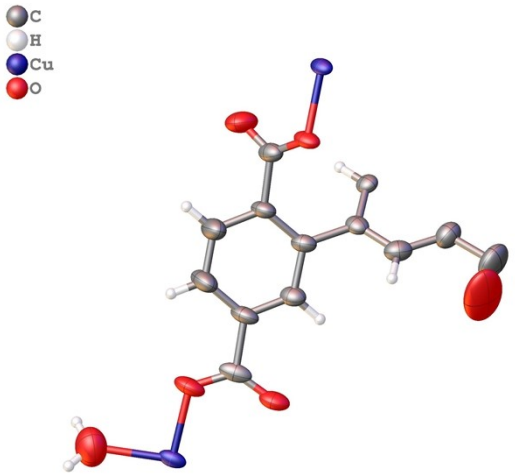

(a)

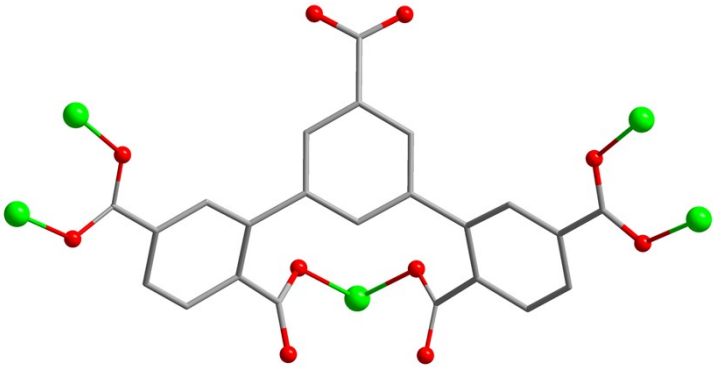

(b)

Fig. S4. 3D microporous framework of **2** and along *c*-axis. All the H atoms and guest molecules are omitted for clarity.

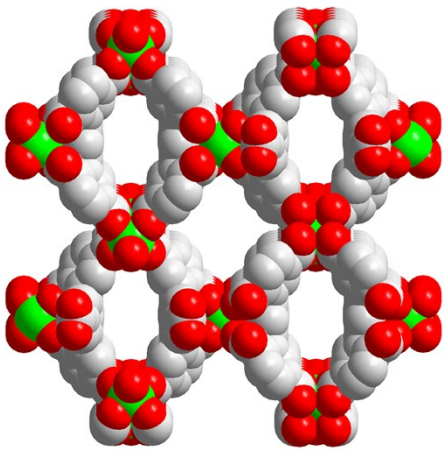

Fig. S5. PXRD patterns of **1-2** in (a-b) simulated from the X-ray single-crystal structure and experimental samples.

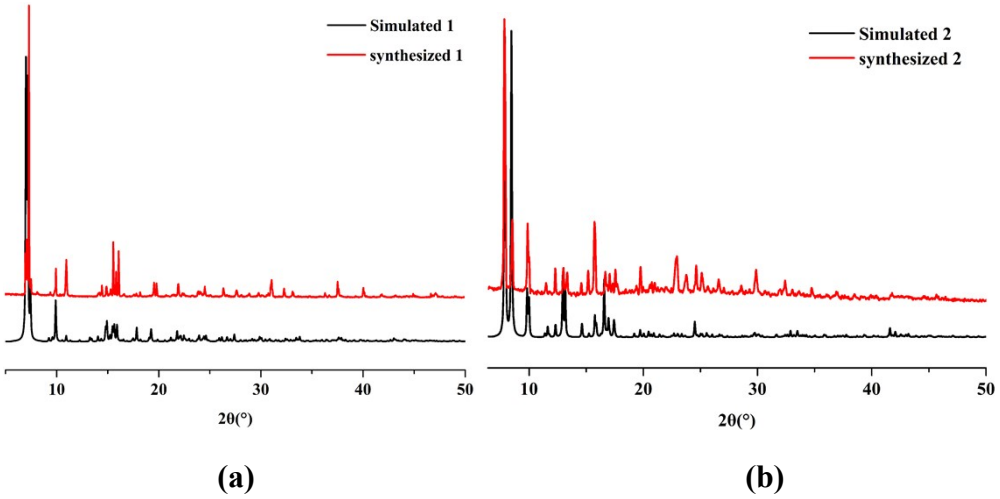

Fig. S6. TGA curves for **1** and **2**.

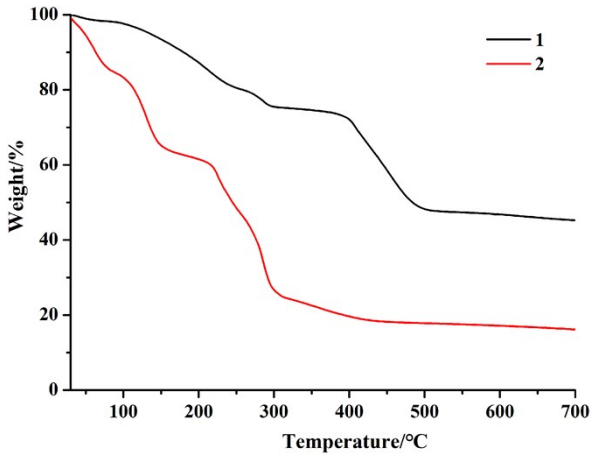

Fig. S7. Luminescence spectra of **1** and free ligand in the solid state at room temperature.

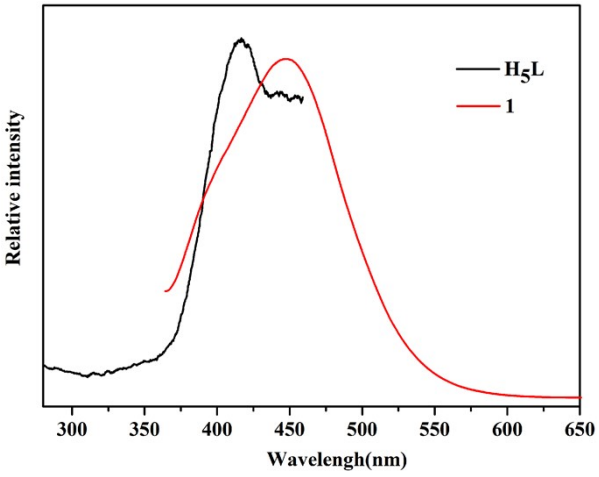

Table S3. Standard Deviation (σ) calculation for the detection of Fe^{3+} for **1.**

Test	fluorescence intensity (nm)
1	1191.774
2	1191.398
3	1190.986
4	1192.047
5	1191.549
average	1191.551
standard deviation (σ)	0.399

Table S4. A comparison of various fluorescent materials used for detecting Fe^{3+}.

Fluorescent materials	Ksv/M^{-1}	detection limit/M	Ref.
CUST-532	1.01×10^4	1.12×10^{-6}	1
$\{[Cd(L)(SDBA)(H_2O)]\cdot 0.5H_2O\}_n$	3.59×10^4	7.14×10^{-6}	2
$\{[Zn(\mu\text{-HCIP})(\mu\text{-pbix})]\cdot 2H_2O\}_n$	6.87×10^3	3.72×10^{-6}	3
BUT-15	1.66×10^4	3.0×10^{-7}	4
Complex **1**	9.799×10^4	1.2×10^{-5}	This work
$Eu(acac)_3 \subset Zn(C_{15}H_{12}NO_2)_2$	-	5×10^{-3}	5
$Eu(C_{22}H_{14}O_2)_3$	-	10^{-4}	6
$\{[Zn(L)(dcdps)]\}_n$	7.004×10^3	6.21×10^{-5}	7
$\{Zn(L)(bdc)\}_n$	9.066×10^3	4.45×10^{-5}	7
$\{[Cd(L)(oba)]\cdot 0.5DMF\}_n$	4.984×10^3	11.52×10^{-5}	7
$\{[Cd(L)(bdc)\cdot 2H2O]\ 2DMF\}_n$	6.387×10^3	6.36×10^{-5}	7

Fig. S8. Multiple cycles for the fluorescence quenching of **1** by Fe^{3+} and recovery after washing by H_2O for several times.

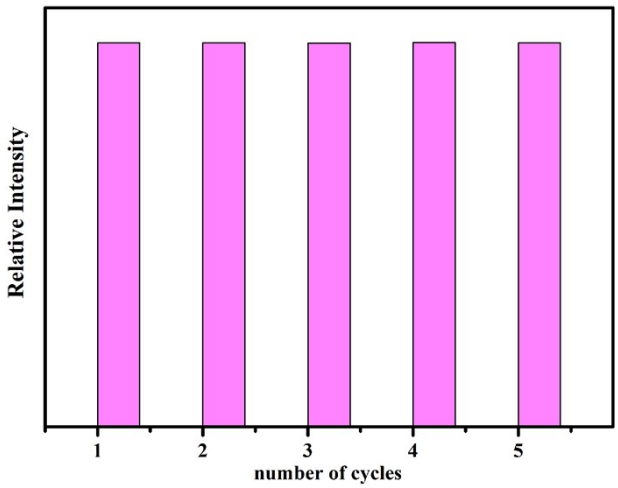

Fig. S9. PXRD patterns of **1** treated by different $M(NO3)_X$ aqueous solutions. It indicated that **1** retains its framework after immersed in aqueous solution containing different cations.

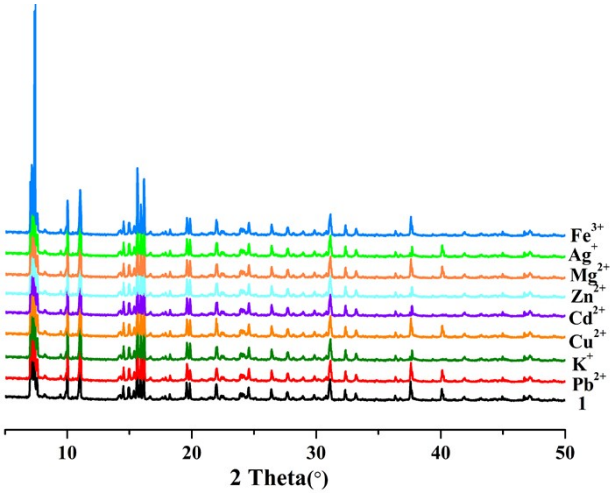

Fig. S10. UV-Vis adsorption spectra of $M(NO_3)_X$ aqueous solutions, the excitation spectrum and the emission spectrum of **1**.

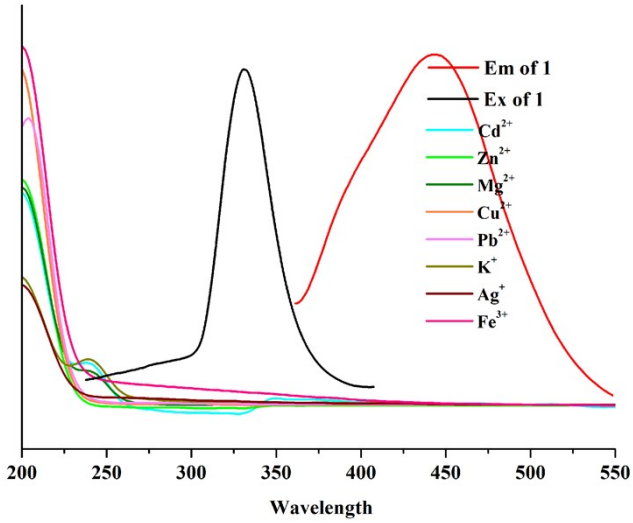

Fig. S11. XPS spectra of O 1s for **1** and Fe^{3+}-**1**.

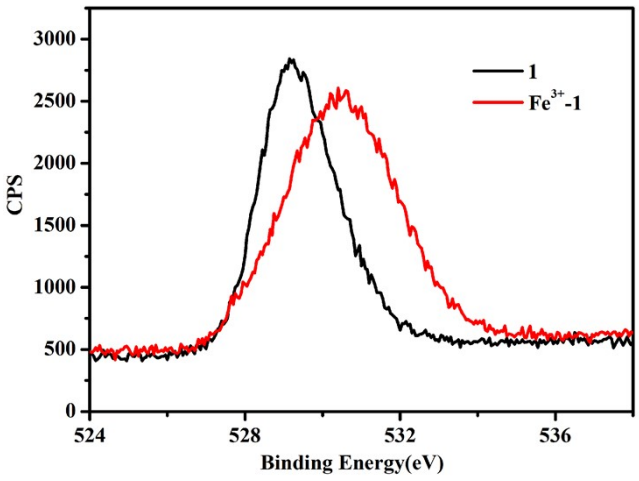

(a)

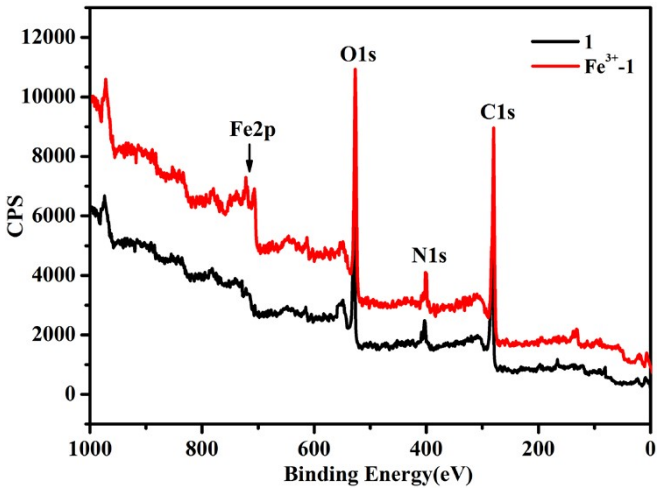

(b)

Table S5. Standard Deviation (σ) calculation for the detection of $Cr_2O_7^{2-}$ for **1.**

Test	fluorescence intensity (nm)
1	1286.365
2	1285.998
3	1287.016
4	1285.899
5	1286.056
average	1286.267
standard deviation (σ)	0.906

Table S6. A comparison of various fluorescent materials used for detecting $Cr_2O_7^{2-}$.

Fluorescent materials	Ksv/M^{-1}	detection limit/M	Ref.
$\{[Zn(L)(dcdps)]\}_n$	4.456×10^4	1.03×10^{-5}	7
$\{Zn(L)(bdc)\}_n$	7.716×10^4	5.55×10^{-6}	7
$\{[Cd(L)(oba)]\cdot 0.5DMF\}_n$	6.145×10^4	7.36×10^{-6}	7
$\{[Cd(L)(bdc)\cdot 2H_2O]\ 2DMF\}_n$	4.248×10^4	1.05×10^{-5}	7
Complex **1**	1.455×10^4	1.86×10^{-4}	This work
$\{[Zn_2(Hbtc)_2(BTD\text{-}bpy)(MeOH)_2]\cdot MeOH\}_n$	6.12×10^3	2.38×10^{-3}	8
$\{[Cd_3(HL)_2(H_2O)_3]\cdot 3H_2O\cdot 2CH_3CN\}_n$	6.99×10^3	1.17×10^{-4}	9
$\{[Zn_2(1,4\text{-}ndc)_2(BTD\text{-}bpy)]\cdot 0.5MeOH\cdot H_2O\}_n$	8.94×10^3	0.75×10^{-3}	8
$[Zn_2(tpeb)(bpdc)_2]$	1.12×10^4	1.04×10^{-3}	10
$[Zn(L)_2]\cdot 2DMF$	1.25×10^4	1.45×10^{-3}	11
$[Zn(pdca)(bbibp)_{0.5}]_n$	8.05×10^3	3.7×10^{-6}	12

Fig. S12. Multiple cycles for the fluorescence quenching of **1** by $Cr_2O_7^{2-}$ and recovery after washing by H_2O for several times.

Fig. S13. PXRD patterns of **1** treated by different K_x(anion) aqueous solutions. It indicated that **1** retains its framework after immersed in aqueous solution containing different anions.

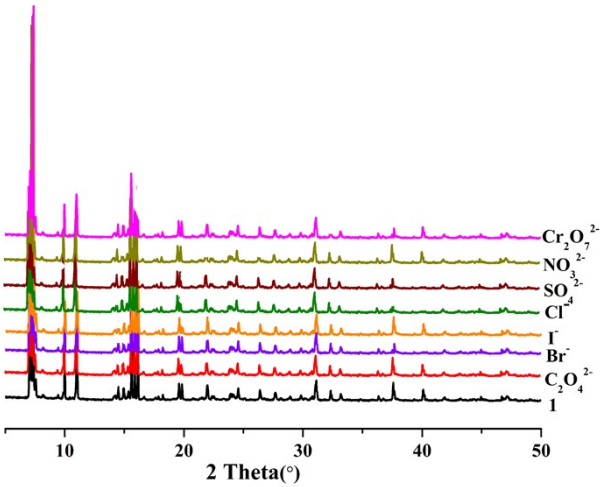

Fig. S14. UV-Vis adsorption spectra of K(anion)x aqueous solutions and the excitation spectrum and the emission spectrum of **1**.

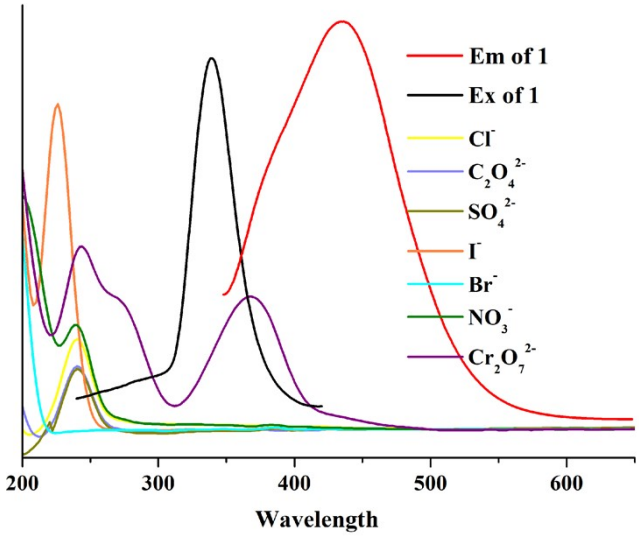

Fig. S15. IR spectra of the as-synthesized **1-2** in (a-b).

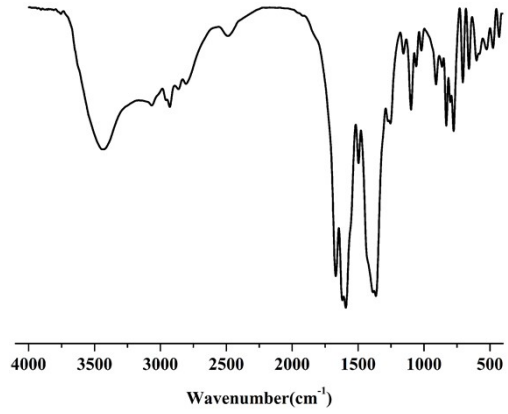

(a)

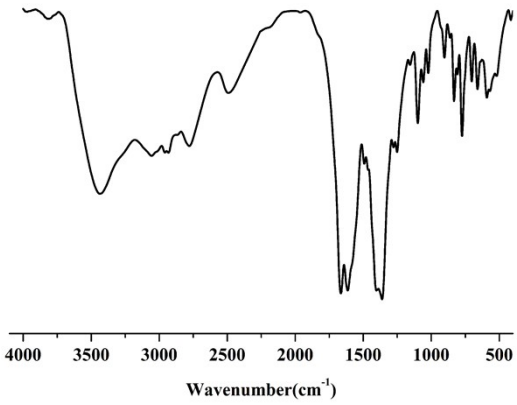

(b)

References

1. M.-Y. Fan, B. Sun, X. Li, Q. Pan, J. Sun, P. Ma, Zhong. Su, *Inorg. Chem*., 2021, **60**, 9148−9156
2. S.-G. Chen, Z.-Z. Shi, L. Qin, H.-L. Jia, H.-G. Zheng, *Cryst. Growth Des*., 2017, **17**, 67−72.
3. M. Arici, *Cryst. Growth Des*., 2017, **17**, 5499−5505.
4. B. Wang, Q. Yang, C. Guo, Y.-X. Sun, L.-H. Xie, J.-R. Li, *ACS Appl. Mater. Interfaces*, 2017, **9**, 10286−10295.
5. Q. Tang, S.-X. Liu, Y.-W. Liu, J. Miao, S.-J. Li, L. Zhang, Z. Shi, Z.-P. Zheng, *Inorg. Chem.*, 2013, **52**, 2799–2801.
6. G.-G. Hou, Y. Liu, Q.-K. Liu, J.-P. Ma, Y.-B. Dong, *Chem. Commun*., 2011, **47**, 10731–10733.
7. F.-Y. Ge, G.-H. Sun, L. Meng, S.-S. Ren, H.-G. Zheng, *Cryst. Growth Des*., 2020, **20**, 1898−1904.

8. Q. J. Jiang, J. Y. Lin, Z. J. Hu, V. K. S. Hsiao, M. Y. Chung and J. Y. Wu, *Cryst. Growth Des*., 2021, **21**, 2056-2067.
9. W. Q. Tong, W. N. Liu, J. G. Cheng, P. F. Zhang, G. P. Li, L. Hou and Y. Y. Wang, *Dalton Trans*., 2018, **47**, 9466-9473.
10. B. B. Rath and J. J. Vittal, *Inorg. Chem*., 2020, **59**, 8818-8826.
11. B. Li, Q. Q. Yan and G. P. Yong, *J. Mater. Chem. C*, 2020, **8**, 11786-11795.
12. D. M. Zhang, C. G. Xu, Y. Z. Liu, C. B. Fan, B. Zhu and Y. H. Fan, *J. Solid State Chem*., 2020, **290**, 121549.